NUMERICAL INVESTIGATIONS OF 1-D AND 2-D CONDUCTION IN THE COUPLING WITH CONVECTION HEAT TRANSFER IN RECTANGULAR DUCTS

Robson Leal da Silva, rlealsilva@hotmail.com
Ezio Castejon Garcia, ezio@ita.br
Instituto Tecnológico de Aeronáutica (ITA) - Divisão Eng. Mecânica-Aeronáutica (IEM)
Pr. Marechal Eduardo Gomes, 50 - Vila das Acácias CEP 12228-900 – São José dos Campos – SP – Brasil

Abstract. *When performs numerical simulations for laminar internal flow with boundary conditions, given by more than one heat transfer mode, considerations for 1-D or 2-D conduction at the walls are evaluated. In this paper, air is considered as working fluid. The walls are considered as small thickness being the analyses done for carbon-steel material. The wall conduction is modeled for horizontal and lateral walls for 1-D analyzes, plus for longitudinal length for 2-D analyze cases. A numerical method of iterative solution is applicable for a system of algebraic equations obtained by finite difference discretization. These equations arises from the energy balance from conduction at the duct walls which is coupled to internal duct convection from the working fluid as well the external convection as boundary conditions. The developed methodology considers non-imposed (or free) wall temperatures in which the heat conduction-convection transfer modes are coupled. It means, the wall mean temperatures and energy balance generates an increasing of the bulk temperature in the working fluid inside of the duct. Even in the present case for non-imposed boundary conditions, fully hydrodynamic and thermal developed internal flows are presents: the temperature field changing in the profiles but keeping the relative shape. Results present the effects on 3-D heat transfer coupling (conduction-convection) in two proposed models for the bulk temperature, wall mean temperature as well as the longitudinal behavior heat rates and variations. These parameters are evaluated in numerical and physical aspects in rectangular duct internal flows.*

Keywords*: heat transfer coupling, numerical methods, thermal systems, heat exchangers, rectangular ducts*

1. INTRODUCTION

Modeling of 3-D thermal conditions for coupling of multi-mode heat transfers (conduction-convection) in ducts of rectangular cross section is being considered in the present work. That corresponds to a heat exchanger, which is a device widely considered in thermal engineering applications. In these occurs heat exchange between two working fluids, being each fluid in one side of a solid wall and with different temperatures.

In heat exchangers simultaneously exists in time and space more than one heat transfer mode. When these are analyzed, the researcher has motivation to look for numerical solutions for the 3-D temperature field and all others parameters based on energy, for example, heat rate, heat transfer convection coefficient, Nusselt number and entropy generation.

Good predictions of heating and/or cooling capacity of those devices are desirable, once these predictions are parameters of major importance in the product developments, to achieve an optimized equipment designs. A structured mesh over the 3-D domain along the three axes is created to implement the computational model of the heat exchanger.

When performs numerical simulations for laminar internal flow, where the boundary conditions are given by more than one heat transfer mode, considerations for 1-D or 2-D conduction at the walls are evaluated. In this paper, air is considered as working fluid. The walls are considered as small thickness being the analyses done for carbon-steel material. The wall conduction is modeled for horizontal and lateral walls for 1-D analyzes, and additionally for the longitudinal length for 2-D analyze case.

Studies of laminar heat transfer in internal flow are widely spreads in available literature. These, for particular cases of analysis for rectangular ducts, are much based on considerations taken in to account done in works of Clark and Kays (1953), Shah and London (1978), and others after them. Constant boundary conditions are usually analyzed, once they represent real situations that occurs for $Tw = constant$ (constant wall temperature in the external fluid phase changing, for example) and for $qw'' = constant$ (constant wall heat flux as happens if we consider external solar radiation in a sunny day, for example). In that line of research, relevant works have also been developed for circular ducts and constant wall temperature or heat flux, as for example by Barozzi and Pagliarini (1985), Faghiri and Sparrow (1980), among others authors in a rather large number of publications available on that subject.

Methodology in the present work considers non-imposed (or free) boundary conditions (wall temperatures or heat flux) in which there is coupling of heat transfer modes. Then, wall mean temperatures are obtained as function of the 3-D temperature field that comes from solving the energy balance at the walls. As consequence, we have increasing values for the bulk temperatures, once the walls together with outside temperatures impose a heating in the internal fluid.

2. GOVERNING EQUATIONS

Considering the flow as laminar, under steady state conditions and neglecting the field forces ($\rho.g$), equations derived from fluid mechanics and heat transfer can represent the proposed model in this work, as indicated by the following: Eq. (1) describes the continuity equation (i.e., mass conservation), Eq. (2) corresponds to the momentum equation and Eq. (3) represents the energy equation.

$$\frac{\partial u}{\partial z} = 0 \tag{1}$$

$$\frac{\partial^2 u}{\partial x^2} + \frac{\partial^2 u}{\partial y^2} = \frac{1}{\mu}.\frac{\partial p}{\partial z} \tag{2}$$

$$\frac{\partial^2 T_f}{\partial x^2} + \frac{\partial^2 T_f}{\partial y^2} = \frac{u}{\alpha}.\frac{\partial T_f}{\partial z} \tag{3}$$

Where u is the velocity, T_f is the fluid temperature; p is the duct internal pressure; dp/dz is a constant value for the pressure gradient at the z direction (axial/longitudinal); ρ is the fluid specific mass (or density); k_f is the fluid thermal conductivity; c_p is the specific heat at constant pressure; μ is the dynamic viscosity; and α is the thermal diffusivity $[\alpha = k_f / (\rho. c_p)]$.

Considering small values for the dynamic viscosity μ, as occurs for fluids as air, we can assume negligible viscous friction due to the work generated from viscous stress. The internal flow is assumed to be in a region of completed development of the velocity distributions (hydrodynamic boundary layer) and temperature distributions (thermal boundary layer). In this situation, although we have a 2-D velocity profile, there exists only the u component at z-axis (unidirectional).

Figure 1 indicates the adopted axes and reference system, as well a considered rectangular duct sketch to apply the governing equations that represent the physical properties of the flow under analysis, at the modeled heat transfer. Also indicated, there are the velocity components w, v and u respectively at axes x, y and z.

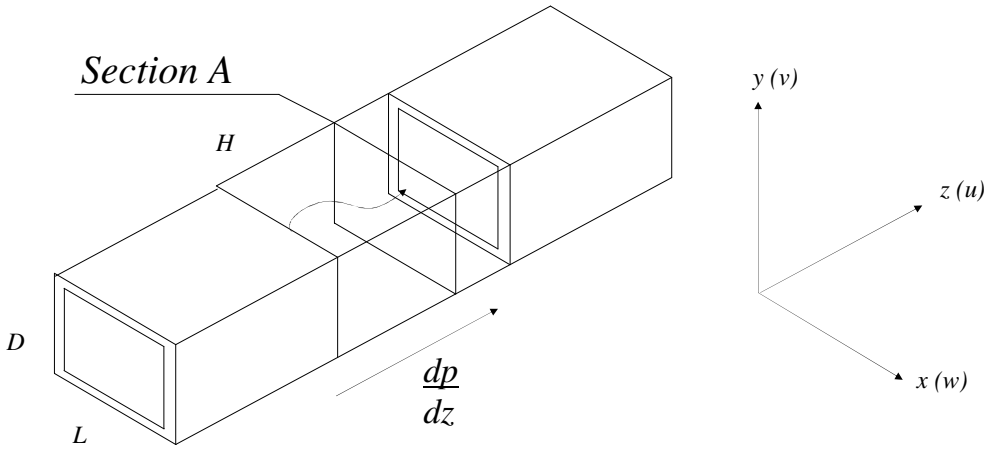

Figure 1. 3-D Rectangular duct flow sketch for conduction-convection coupling.

Formulation originally developed by Clark e Kays (1953) are applicable to rectangular cross section ducts, which considers boundary conditions at the walls with imposed constant temperatures at the cross section under analysis and along the duct length (flow direction). According to developments performed by Garcia (1996), it is possible to define a value that represents the mean wall temperatures in a given cross section T_{Wm}, Eq. (4). Then, it is possible to develop similarly to the original formulation, resulting in a new expression for the energy equation, as show in Eq. (5).

$$T_{Wm} = \frac{\left[\frac{1}{L}.\int_0^L T_1(0,y).dy + \frac{1}{D}.\int_0^D T_2(x,0).dx + \frac{1}{L}.\int_0^L T_3(D,y).dy + \frac{1}{D}.\int_0^D T_4(x,L).dx\right]}{4} \tag{4}$$

$$\frac{\partial^2 T_f}{\partial x^2} + \frac{\partial^2 T_f}{\partial y^2} = \frac{u}{\alpha}.\left(\frac{Tw_m - T_f}{Tw_m - T_b}\right)\frac{\partial T_b}{\partial z} \tag{5}$$

In the present work, 3-D results are obtained by solving the system of equations for a given cross section ($z = n$) and then solved to forward cross sections ($z = n+1$), in which T_{Wm} is still considered of constant value at each cross section, but with different values in each one.

The following considerations are applicable to previous formulation, in the transformation of main parameters (or variables) to their dimensionless forms:

$$X = \frac{x}{D_h}, \qquad Y = \frac{y}{D_h}, \qquad V = \frac{u}{U_b} \qquad \text{and} \qquad \phi = \frac{a.(T_{Wm} - T_f)}{U_b.D_h^2.\left(\frac{dT_b}{dz}\right)} \tag{6), (7), (8) and (9)}$$

After some mathematical developments (replacing and rearranging of governing equations), in which are available in recent works from Silva and Garcia (2006a and 2006b), equations for the dimensionless energy equation and dimensionless bulk temperature are obtained as indicated, respectively, by Eq. (10) and (11).

$$\frac{\partial^2 \phi}{\partial X^2} + \frac{\partial^2 \phi}{\partial Y^2} = -V.\frac{\phi}{\phi_b} \tag{10}$$

$$\phi_b = \frac{D_h^2}{A}.\iint V.\phi.dX.dY \tag{11}$$

It is possible to compute the heat transfer rate per length unit, Eq. (12). It depends on values for T_{wm} and average heat convection coefficient, or from fluid enthalpy derivative [$dh_b = c_p.dT_b$], given from the temperature bulk gradient dT_b/dz, as presented in the Eq. (13).

$$q^{`} = P_e.\bar{h}.(T_{Wm} - T_b) \tag{12}$$

$$q'_f = \rho.U_b.A.c_p.\frac{dT_b}{dz} \tag{13}$$

When makes equal Eq. (12) and (13), it is possible to unfold the resulting expression, in which is applied integration between two cross sections: inlet (namely z_1) and outlet (namely z_2), resulting in Eq. (14).

$$T_{b_{z2}} = T_{Wm} - (T_{Wm} - T_{b_{z1}}).e^{-\left(\frac{P_e}{2A}\right)^2.\frac{a}{U_b}.N_u.(z_1 - z_2)} \tag{14}$$

From Eq. (14), we obtain the bulk temperature longitudinal (z-axis) variation ΔT_b when cutting the duct in a lot of segments and applying the numerical method to solve the properties in each finite cross section. For a given bulk temperature value at the duct inlet section (T_{b1}), after solving the system of equations, bulk temperature at the duct outlet (T_{b2}) is computed from that expression. Then, making $T_{b1}=T_{b2}$, there is a new T_{b1} (as initial condition) applicable to the next segment/cross section, and there is an update on boundary conditions, dimensionless temperature field distribution (ϕ) and dimensionless bulk temperature (ϕ_b), as indicated in Eq. (10) and (11).

2.1. Boundary and Inlet Conditions

Non-dimensional boundary conditions are given by the following equations:

$$\phi(0,Y)=\frac{\alpha.(T_{Wm}-T)}{U_b.D_h^2.\left(\frac{dT_b}{dz}\right)} \quad \text{and} \quad \phi(X,0)=\frac{\alpha.(T_{Wm}-T_2)}{U_b.D_h^2.\left(\frac{dT_b}{dz}\right)} \tag{15}$$

$$\phi(^{D}/_{D_h},Y)=\frac{\alpha.(T_{Wm}-T_3)}{U_b.D_h^2.\left(\frac{dT_b}{dz}\right)} \quad \text{and} \quad \phi(X,\tfrac{L}{D_h})=\frac{\alpha.(T_{Wm}-T_4)}{U_b.D_h^2.\left(\frac{dT_b}{dz}\right)} \tag{16}$$

If we consider constant temperatures at the walls, Eq. (15) and (16) being equal to zero, for these particular conditions it is possible to notice that boundary conditions are not function of dT_b/dz. That simplification becomes equal to the one studied by Patankar (1991). Equation (11) and its derivations for dimensional values of T_b and T_f (Silva and Garcia, 2006a), as well as boundary conditions from Eq. (15) and (16), make together a set of differential equations in which ϕ and dT_b/dz parameters are unknown. When solving that equation system it is possible to obtain the temperature field distributions, T_f.

In a fully developed flow, velocity distributions reach maximum values at the central section and zero values at the walls, due to non-slipping conditions. Pressure gradient between inlet and outlet duct cross sections, *dp/dz* at Eq. (2), is an imposed value that is in accordance to laminar flow conditions (low Reynolds number). Fluid bulk temperature T_b is defined for inlet air flow in ambient conditions at 300K, being the changes along the duct length obtained by energy balance that considers heat transfer rates due to conduction and convection in each wall finite element (Fig. 2).

Table 1 indicates the initial set-up variables/parameters for internal and external conditions, including geometry dimensions and pressure gradient considered to obtain laminar fluid flow *(Re < 2100).*

Table 1. Fluid flow parameters and rectangular duct geometry.

Tb_inlet (K), entrance	300
Te (K), external temperature for case 1	300
Te (K), external temperature for case 2	350
he (W/ m².K), external convection heat transfer coefficient	12
α, aspect ratio*	1
D (m), duct high	0.01
L (m), duct width	0.01
Z, non-dimensional duct length*	1.00
dp/dz (Pa/m) (1)	16.00

(1) *Pressure gradient to keep laminar fluid flow, considering air and α* = 1.*

2.2. Thermo-physical properties

The heat exchanger shown in Fig. 1 is built in four solid walls (rectangular duct geometry) according to material properties in Tab. 2, and the internal fluid (in this case, air) flow in conditions pointed out in Tab. 3. In this work, all results refer to carbon steel building, and future work will look into the behavior for the three others.

Table 2: Wall material thermo-physical properties (1) (Incropera and De Witt, 1998).

	k (W / m.K)
Stainless Steel	13.4
Carbon Steel (Mn≤1%; Si≤0.1%)	60.5
Pure Aluminum	237.0
Pure Copper	401.0

(1) *material at 300K.*

When computing internal convection (to any fluid as air, water or oil), it is necessary to obtain local coefficients at the walls, *h=f(x,y)*. For external convection (air) it is considered global coefficients (*h_external*, Tab. 1), according to the working fluid outside the duct walls, to obtain representative results in a heat exchanger, according to the inside working fluid properties pointed out in Tab. 3.

Table 3. Fluid Properties for internal flow [(1)] (Moran et al, 2005)

Parameter description	S.I. Symbols and Units	Numerical Value
Specific heat	c_p (kJ/kg.K)	1005.7
Specific mass	ρ (kg/m^3)	1,1614
Thermal conductivity	k_f (W/m.K)	2.63 x 10^{-2}
Thermal diffusivity	α (m²/s)	225 x 10^{-7}
Dynamic viscosity	μ (N.s/m²)	1.846 x 10^{-5}

(1) *air at 300K.*

2.3. Energy balance at the walls for 1-D and 2-D conduction models

An analysis of one infinitesimal element located at the duct walls, according to Fig. 2, allows performing an energy balance that will provide the relations between the heat fluxes from all the heat transfer modes existing in the model, that is, conduction-convection coupling as a function of non-imposed temperature distributions on the walls.

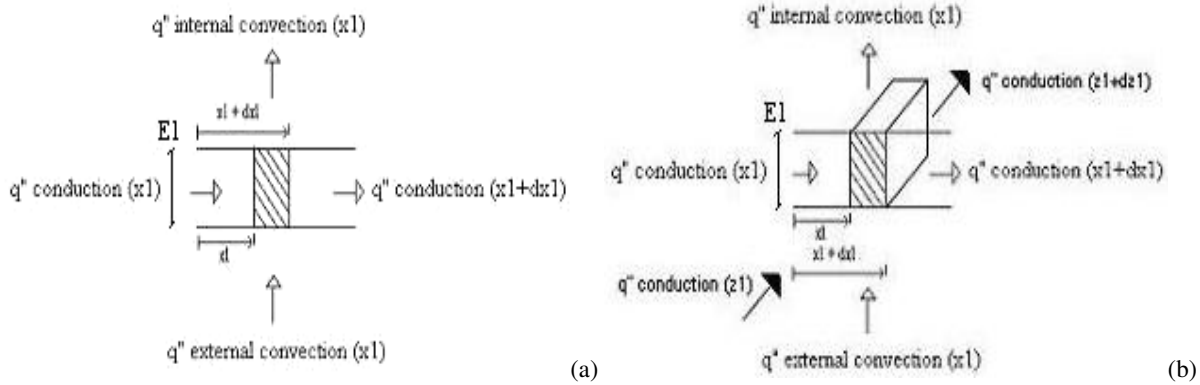

Figure 2. Energy balance for 1-D (a, left) and 2-D (right, b) conduction and convection at wall surface 1 (bottom-T_1).

Thus, from energy conservation principle, for steady state conditions, the heat rate quantities that get into the finite element must be equal to the quantities that get out, that is, for a given wall (number 1 corresponds to the bottom in Fig. 1), we have the resulting balance described in Eq. (17). Similar equations and energy balance can be obtained when applying to walls 2, 3 and 4 considering that external convection occurs in walls 1 and 3, under symmetry conditions considered on the walls 2 and 4 (at all duct, side by side).

$$\begin{aligned} &q''_{cond_1}(z_1).dz_1.E_1 + q''_{cond_1}(x_1).dz_1.E_1 + q''_{convec\_ext_1}.dx_1.dz_1. = \\ &q''_{cond_1}(z_1+dz_1).dx_1.E_1 + q''_{cond_1}(x_1+dx_1).dx_1.E_1 + q''_{convec\_int_1}.dx_1.dx_1 \end{aligned} \tag{17}$$

Unfolding Eq. (17), the following relation appears:

$$\begin{aligned} &\left[-k_1.\frac{dT_1}{dz_1}\right].E_1 + \left[-k_1.\frac{dT_1}{dx_1}\right].E_1 + \{h_{ext}.(x_1).[T_1(x_1)-T_{ext}]\}.dx_1 = \\ &\left[-k_1.\frac{dT_1}{dz_1} - k_1.\frac{d^2T_1}{dz_1^2}.dz_1\right].E_1 + \left[-k_1.\frac{dT_1}{dx_1} - k_1.\frac{d^2T_1}{dx_1^2}.dx_1\right].E_1 + \{h_1.(x_1).[T_1(x_1)-T_{b\_int}]\}.dx_1 \end{aligned} \tag{18}$$

Finally, we have:

$$k_1.\frac{d^2T_1}{dz_1^2}.dz_1.E_1 + k_1.\frac{d^2T_1}{dx_1^2}.dx_1.E_1 = +h_1.(x_1).[T_1(x_1) - T_{b\_\text{int}}].dx_1 - h_{ext}.(x_1).[T_1(x_1) - T_{ext}].dx_1 \quad (19)$$

Equations (17) up to (19) correspond to energy balance in the 2-D conduction model, Fig. 2(b), were conduction heat transfer is considered in two directions (*x* and *z*-axes). Equations for 1-D conduction model, where only conduction heat transfer in one direction (*x-axis*) is considered, is obtained if we consider *dT/dz* equal to zero, that is no conduction in *z*-axis direction.

3. COMPUTATIONAL AND NUMERICAL SOLUTION ALGORITHM

After applying the method of finite differences on the algebraic equations obtained for velocity and temperature fields, they are solved using Gauss-Seidel methodology. Discretized equations, obtained from energy balance that represents the conduction and convection heat transfer coupling at the walls (Fig. 2), are solved by using an adapted TDMA method (Patankar,1991 and Garcia, 1996).

After a first evaluation of the properties at initial cross section (*z=0*), the entire computational domain (up to *z=H*) is submitted to cyclic evaluation until obtain convergence for the dimensionless temperature distributions, *Ø*.

The following seven steps indicate the developed and applied methodology in the numerical solution:

Step1: Obtain velocity field and set up of initial estimated values for T_{Wm} *and* dT_b/dz;

Step 2: Equations for the thermal boundary conditions are evaluated (Eq. 15 and 16);

Step 3: Dimensionless energy equation (Temperature field, *Ø*) at Eq. (10) is solved and $Ø_b$ is computed according to Eq. (11), until convergence is obtained ($Ø_b$ < tolerance), what ends the first iterative loop;

Step 4: A value for dT_b/dz is computed by putting that parameter in evidence at Eq. (11) and then returns to step 2 where boundary conditions are updated to obtain a new solution for the temperature field (step 3), until convergence is obtained (dT_b/dz< tolerance), what ends the second iterative loop;

Step 5: *Ø(n)* obtained is then used as assumption values for *Ø(n+1) = Ø(n)*, which is required for iterative solution of the 2-D conduction in the energy balance at the walls, and also required if values for *Ø(n-1),* that is acquired from step 3 in the first calculation loop;

Step 6: A new value for T_f is computed, according to Eq. (10) rearranged to its dimensional form (Silva and Garcia, 2006a), what provides all information that is required to compute the temperature gradient between two duct cross sections and also the bulk temperature in next section, $T_b(n+1)$. That continues until *z=H*;

Step 7: Computation of updated values for *Ø (n=2 up to the end*) and comparison to previous values until convergence is obtained, i.e., (Ø_updated - Ø_previous) < tolerance, what finishes the third and last iterative loop otherwise the solution algorithm returns to step 2.

At the steps, tolerance of 10^{-5} is the value to be accomplished by the convergence criteria applicable to $Ø_b$ (fluid flow dimensionless bulk temperature), dT_b/dz (dimensional bulk temperature gradient between two cross sections) and *Ø_updated (*dimensionless temperature field in all points of the computational model*)*.

4. RESULTS

Two kinds of external conditions (outside boundary) were taken into account in the conduction model analysis and its corresponding results: a) *Te = 300K*, and constant heat flux from outside the walls (*qe" = 1100 W / m²*); b) *Te = 350K* and no heat flux considered (*qe" = 0*), what corresponds conduction - internal convection effects, only. In both cases, we have boundary conditions at the walls with free values i.e., non-imposed temperature or heat flux, which will converge to temperature distributions values according to the energy balance (conduction-convection) iterative solution at the rectangular duct perimeter. Temperature distributions in the entire field (inside duct walls) are also available, as consequence of numerical convergence of the energy conservation equation.

Obtained results are then compared to each other in a quantitative and qualitative analysis. This allows a good prediction of how much is the increase in terms of degree for the temperature distributions and the necessary length for the fluid flow reach a given temperature value for the geometric parameters in a certain heat exchanger.

4.1. Heat rate analysis

Figure 3 presents the heat rate (*q'*) received by the internal flow (that is different of the outside heat flux, *qe"*) along the rectangular duct length (*z-axis*, longitudinal direction) for the two outside conditions mentioned previously.

For both external conditions, it is possible to notice that the internal fluid flow receives an incoming heat flux higher for 1-D conduction modeling when compared to the values in 2-D conduction modeling. The reason becomes clear when comparing 1-D and 2-D results for outside *qe"=constant* (that is the closest approach to literature results for constant heat flux as boundary condition at the walls). For 1-D conduction model, the energy path goes from the

outside, crosses the walls in the thick direction and reaches the fluid flow, while in 2-D conduction part of the same amount of outside energy goes to the walls at the longitudinal direction.

In 2-D model, energy conservation is also fulfilled and the heat transfer effects approach closer to real and practical conditions that occur in engineering applications, as indicated by next results.

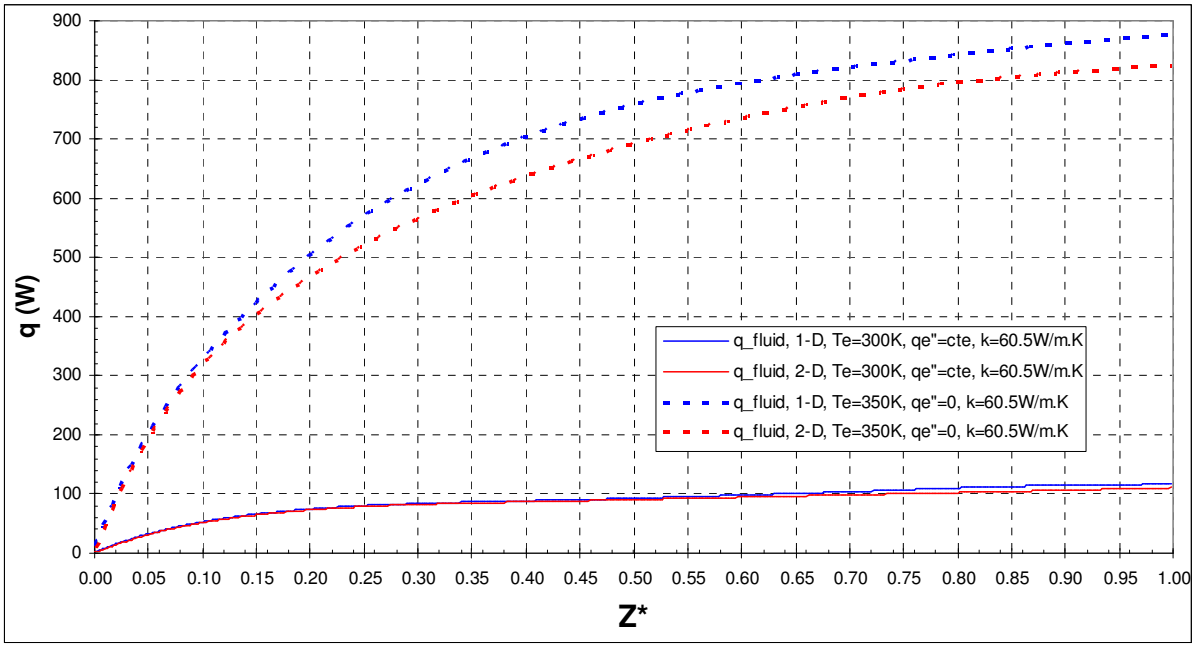

Figure 3. Heat rate received by the working fluid along longitudinal direction – carbon steel walls.

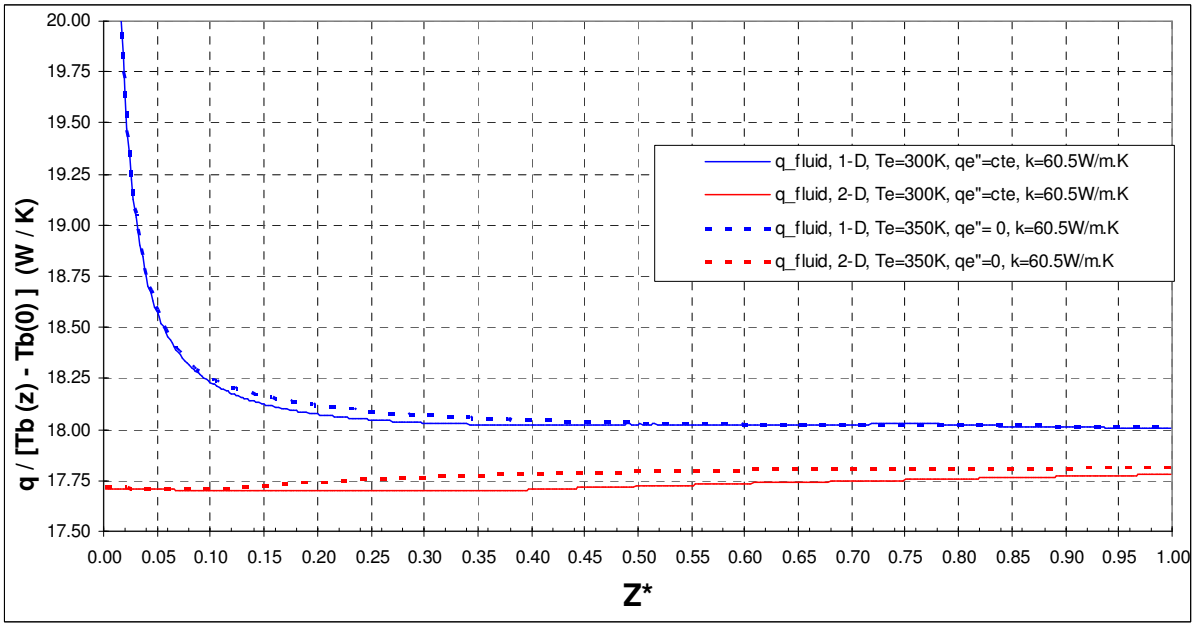

Figure 4. Required heat rate to increase one Kelvin degree in the internal fluid temperature – carbon steel walls.

Figure 4 shows the same parameter indicated in Fig. 3, i.e., heat rate *(q)* but here divided by fluid bulk temperature variations $[T_b(n) - T_b(0)]$, resulting in a parameter that is given by (W / K) as indicated in the vertical axis of that figure.

An interesting behavior is observed in Fig. 4, which allows a focus on the physical behavior of the heat transfer coupling phenomena under analysis. For 2-D conduction, there is an almost constant heat rate required to increase in one Kelvin degree the fluid temperature, while in the 1-D conduction, that same parameter shows an asymptotic

behavior (reaching infinity) at the beginning lengths and after that, it goes to almost constant values as in 2-D conduction.

Discontinuities as the one observed for 1-D conduction modeling indicates a lack between numerical results and the real phenomena that is not being well represented. Otherwise, it would mean that to increase one Kelvin degree (a unitary value) in the fluid bulk temperature in the region from $z = 0\ m$ up to around $z = 0.25\ m$ requires an amount of energy/heat rate that approaches the infinity, and that does not make sense in the real word. That effect seems to correspond only to numerical response to the 1-D conduction and convection heat transfer coupling under analysis.

In the other hand, 2-D conduction modeling shows a smooth behavior indicating that its results fit better to the real phenomena in the according of available experimental results.

It is good to remember that equations for heat rate can be rearranged in the following form: $q / \Delta T = \dot{m} \, . \, c_p$, where $\dot{m}$ is the mass flow *(kg/s)*, and once $\dot{m}$ and c_p are assumed constants along the flow, it is reasonably to expect that the left hand side $q / \Delta T$ would also be constant. It is also known that heat transfer behavior occurs in smooth and not in rough ways, what also reinforces that 2-D is a better conduction model than 1-D. It gives importance for the research line pursued by authors, and stimulates to continue the studies in rectangular duct heat exchangers.

Also, it is important to point out that case study 1 corresponds to *qe" = constant*, i.e., constant heat flux outside the whole duct length and that condition does not reflect the asymptotic behavior that happens in curves for 1-D model at Fig. 4 (heat rate q divided by $[T_b(n) - T_b(0)]$, in W / K).

In analogy to real conditions, 1-D model corresponds to a duct where each infinitesimal cross section is thermally isolated from its neighborhood, and then heat transfer by conduction does not reach front and rear sides. In 2-D modeling, there is communication among all infinitesimal elements of the rectangular duct in the longitudinal length and in width (left and right walls) or high (top and bottom walls), although it was neglected in the thin wall direction (if considered, that would corresponds to 3-D conduction modeling).

4.2. Temperature analysis

Next figures present non-dimensional temperature gradients in the fluid flow ($\psi_b = T_b / T_{b\_inlet}$) and at the walls ($\psi_W = T_{wm} / T_{b\_inlet}$) along the duct length. In addition, they present the temperature field (dimensional values) along the entire duct computational domain for 1-D and 2-D conduction models and each one of the cases considered, for the same external conditions.

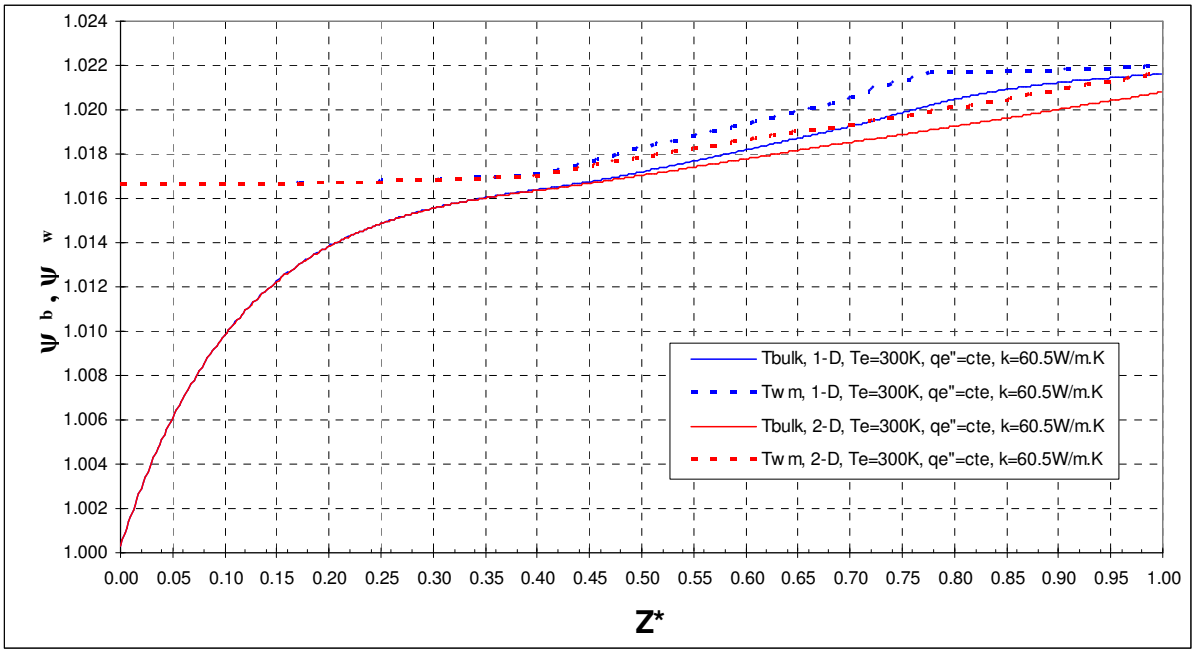

Figure 5. Non-dimensional temperatures behavior for case study 1 – *qe" = constant* and *Te = 300K*.

Figure 5 shows T_b and T_{wm} when *qe" = constant* (1100 W / m²), and *Te = 300K*, where the differences between 1-D and 2-D conduction models begin visually to became noticeable around $z = 3\ m$ for T_{wm}, and around $z = 3.5\ m$ for T_b. That behavior is enhanced up to the duct exit.

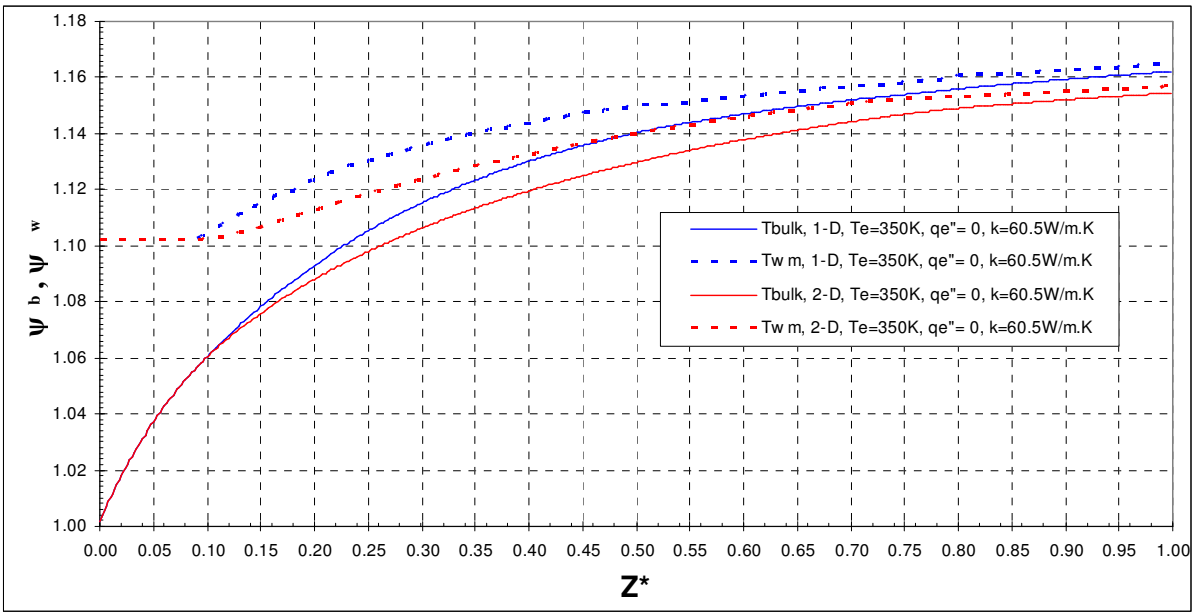

Figure 6. Non-dimensional temperature behavior for case study 2 – *qe" = 0* and *Te = 350K*.

Figure 6 shows the same parameters when *qe" = 0* and *Te = 350K*, where the differences appear closer to the inlet (earlier in length space), indicating that these outside conditions provide higher energy than the previous one. In both figures, T_{wm} does not change much at the beginning of the duct length, indicating that the energy balance into the walls keeps that parameter almost constant.

That conclusion makes sense if we think that the walls are only necessary to serve as a physical mean path between heat energy and inside fluid, which is the one that needs to receive energy represented by temperature increases, what happens since the inlet. It is possible infer that for other materials, with higher thermal conductivity values (k), that behavior is altered, once the material at the walls will conduct as much energy as its thermal conductivity increasing.

Now, with focus on the entire temperature field, Fig. 7 shows results for case study 1. Notice that values for temperature range are from 297K up to 306K. Conduction Model 1-D, at the left side, clearly shows a larger duct length (at the ending) with higher values for temperature distributions, while 2-D conduction model at the same region shows a smaller duct length for the equal temperature values (around 306K). That behavior occurs for all iso-surfaces of temperatures in the Fig. 7, but it intensifies after the middle length, what is consistent to the results indicated in Fig. 5.

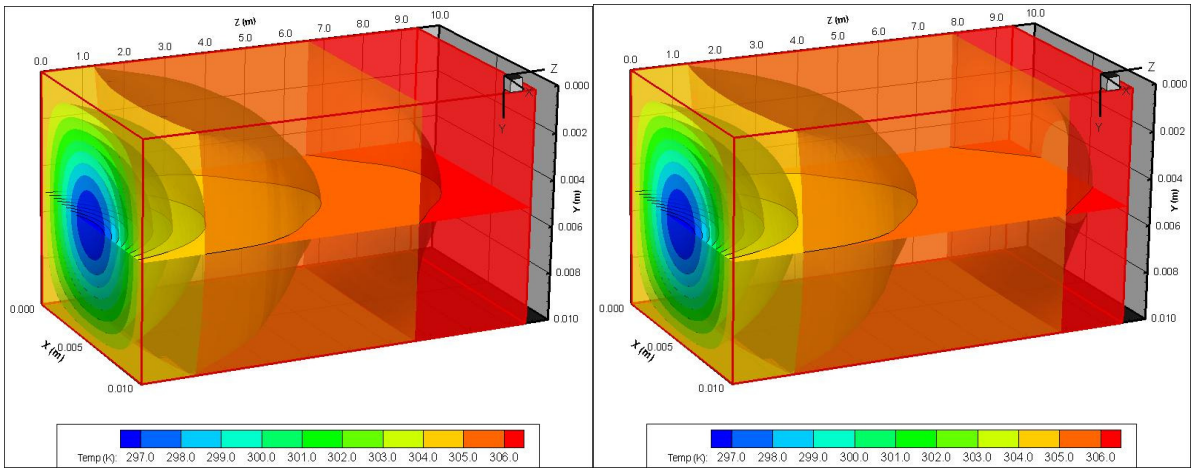

Figure 7. 1-D (left) and 2-D (right) heat conduction modeling case study 1 – *qe" = constant* and *Te = 300K*.

Figure 8 presents the temperature field for case study 2. For this case, temperature range is from 285K up to 345K. The same behavior is observed when compares themselves, 1-D and 2-D conduction models for non-dimensional T_b and T_{wm} along the z-axis in Fig. 6, with increased differences when compared to results in Fig. 7. That occurs due to the higher heat amounts that comes from outside conditions when *qe"=0* and *Te=350K*.

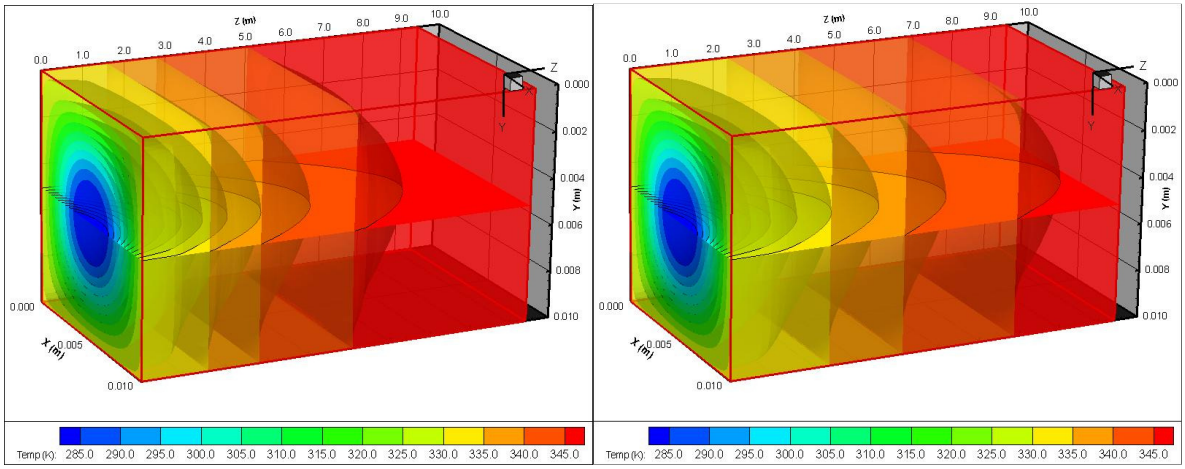

Figure 8. 1-D (left) and 2-D (right) heat conduction modeling for case study 2 – $qe'' = 0$ and $Te = 350K$.

5. CONCLUSIONS

Some achievements were obtained in this work when compared to previous ones by the same authors (Silva e Garcia, 2006a, 2006b and 2007), mainly represented by 2-D heat transfer conduction in 3-D rectangular ducts which wall temperatures are not imposed. That represents a development in the research line followed in the subject, in which corresponds to better modeling of practical conditions found in engineering equipment and real thermal conditions were multi-mode heat transfer occurs. It is not always that improves in the model (1-D to 2-D analysis) will represent an increase in exchanged heat. Notice that 1-D wall conduction is a simplified model that indicates a higher amount of heat reaching the fluid flow. These final notes are the main conclusions of numerical investigations conducted herein.

Analysis of others results are going to be published, using the same behavior of the 1-D and 2-D models. In this future publication, others wall material analysis, as stainless steel, pure aluminum and pure cooper will be done to compare with carbon-steel, here considered. Next steps, in that line of work, are to consider viscous dissipation effects in the energy equation, what provides an additional amount of energy to the fluid flow (usually neglected), and to include radiation heat transfer as part of the heat transfer coupling at the walls. Previous, actual and future works and considerations related herein are going to be part of the first author thesis to obtain its doctors degree expected for 2007.

6. REFERENCES

Barozzi, G.S. and Pagliarini, G., 1985, “A Method to Solve Conjugate Heat Transfer Problems: The Case of Fully Developed Laminar Flow in a Pipe”, ASME Journal of Heat Transfer, Vol. 107, pp. 77-83.

Clark, S.H., and Kays, W.M., 1953, “Laminar Flow Forced Convection in Rectangular Tubes”, Transactions of ASME, Vol. 10, pp. 859-866.

Faghiri, M. and Sparrow, E.M., 1980, “Simultaneous Wall and Fluid Axial Heat Conduction in Laminar Pipe-Flow Heat Transfer”, ASME Journal of Heat Transfer, Vol. 102, pp. 58-63.

Garcia, E.C., 1996, “Condução, Convecção e Radiação Acopladas em Coletores e Radiadores Solares”, ITA-Tese de Doutorado, São José dos Campos, Brasil.

Incropera, F.P., De Witt, D.P.,1998,“Fundamentos de Transferência de Calor e Massa”, Ed.LTC, Rio de Janeiro, Brasil.

Moran, M.J. et al, 2005, “Introdução à Engenharia de Sistemas Térmicos: Termodinâmica, Mecânica dos Fluidos e Transferência de Calor”, Ed. LTC, Rio de Janeiro, Brasil.

Patankar, S.V., 1991, "Computation of Conduction and Duct Flow Heat Transfer", Innovative Research, Maple Grove, USA, 354 p.

Shah, R.K. and London, A.L., 1978, “Laminar Flow Forced Convection in Ducts”, Advances in Heat Transfer, Academic Press, New York, USA.

Silva, R.L., and Garcia, E.C., 2006, “Simulação Numérica do Acoplamento 3-D da Condução-Convecção para Escoamentos em Dutos Retangulares”, 11º ENCIT – Encontro Nacional de Ciências Térmicas, Curitiba-PR, Brasil.

Silva, R.L., and Garcia, E.C., 2006, “Efeito da Razão de Aspecto sob Análise 3-D em Dutos Retangulares com Paredes de Temperaturas Não-Uniformes”, 16º POSMEC – Simpósio Pós-Graduação Eng Mecânica, Uberlândia-MG,Brasil.

Silva, R.L., and Garcia, E.C., 2007, “Temperature and Entropy Generation Behavior in Rectangular Ducts with 3-D Heat Transfer Coupling (Conduction and Convection)”, International Communications in Heat and Mass Transfer.

7. RESPONSIBILITY NOTICE

The authors are the only responsible for the printed material included in this paper.